Molecular Crystals and Liquid Crystals

ISSN: 1542-1406 (Print) 1563-5287 (Online) Journal homepage: http://www.tandfonline.com/loi/gmcl20

Wavelength-tuneable laser emission from a dye-doped achiral nematic liquid crystal dispersed into a chiral polymer scaffold

Simon M. Wood, Steve J. Elston & Stephen M. Morris

To cite this article: Simon M. Wood, Steve J. Elston & Stephen M. Morris (2016) Wavelength-tuneable laser emission from a dye-doped achiral nematic liquid crystal dispersed into a chiral polymer scaffold, Molecular Crystals and Liquid Crystals, 632:1, 89-96

To link to this article: http://dx.doi.org/10.1080/15421406.2016.1185587

Published online: 17 Aug 2016.

MOLECULAR CRYSTALS AND LIQUID CRYSTALS
2016, VOL. 632, 89–96
http://dx.doi.org/10.1080/15421406.2016.1185587

Taylor & Francis
Taylor & Francis Group

Wavelength-tuneable laser emission from a dye-doped achiral nematic liquid crystal dispersed into a chiral polymer scaffold

Simon M. Wood, Steve J. Elston, and Stephen M. Morris

Department of Engineering Science, University of Oxford, Oxford, UK

ABSTRACT

We compare the emission characteristics of a thin-film liquid crystal (LC) laser created using a polymer-stabilized, dye-doped chiral nematic LC to that of an LC laser that was fabricated using an achiral, dye-doped nematic refilled into a chiral polymer scaffold that was templated from the same chiral nematic host. Both lasers exhibit wavelength tuning upon the application of an external electric field. However, for the templated sample, tuning is found to occur across a broader wavelength-range for the same electric field amplitude. We discuss the benefits of the templated approach and how it can be used to circumvent dye bleaching that may occur during photo-polymerisation.

KEYWORDS

chiral nematic liquid crystals; lasers; reactive mesogens

A widely-wavelength tuneable laser with small physical dimensions that may be manufactured in a manner suitable for mass-production would have a wide variety of potential applications ranging from displays [1] to biomedical diagnostic techniques [2]. Liquid crystal (LC) lasers potentially offer these characteristics as they have small cavity dimensions (∼μm thick), relatively low excitation threshold fluences and can be tuned in terms of the emission wavelength [3]. Such lasers are usually based upon the chiral nematic (cholesteric) LC (CLC) phase, but research has also shown that they can be fabricated using the chiral smectic C phase as well as blue phases I and II [4–6].

One of the benefits of using LCs as a photonic band edge laser [7] is that they naturally self-assemble into periodic structures through the formation of macroscopic helices. This, combined with their inherent optical anisotropy, results in the appearance of a 1-dimensional photonic band-gap (PBG) for visible light [8–9]. As substantial research has already shown, these materials can be made to act as lasers by exploiting the large density of photonic states that exists at the edges of the PBG due to the decaying group velocity and the increase in photon dwell time [10]. The wavelengths that define the lowest threshold resonant modes are located at either side of the band gap (i.e. the band-edges) and are determined by the pitch of the helix and the refractive indices parallel and perpendicular to the director, as described by equations 1 and 2 [9]:

$$\lambda_{\mathrm{L}} = n_e p \tag{1}$$

$$\lambda_{\mathrm{S}} = n_o p \tag{2}$$

CONTACT Dr. Stephen M. Morris stephen.morris@eng.ox.ac.uk Department of Engineering Science, University of Oxford, Parks Road, Oxford OX1 3PJ, UK.

Color versions of one or more of the figures in the article can be found online at www.tandfonline.com/gmcl.

This work has not been published elsewhere and it has not been submitted simultaneously for publication elsewhere.

where λ_X is the wavelength-position of the long (X = L) or short (X = S) band-edge of the PBG, n_e and n_o are the refractive indices parallel and perpendicular to the director, respectively, and p is the pitch of the helix. As these equations show, wavelength tuning of the laser emission may be achieved by altering either the relevant refractive index or the pitch of the helix. Both factors are sensitive to a variety of external stimuli, including temperature [11], magnetic fields [12], mechanical deformations [13] and electric fields [14–19].

In terms of electric fields, it is well-known that the direction of the applied electric field relative to the orientation of the helix axis dictates the subsequent response of the CLC. For a CLC with a positive dielectric anisotropy aligned in the uniform standing helix (Grandjean) texture, the application of an electric field perpendicular to the helix axis results in an unwinding of the helix and an elongation of the pitch. Experimentally, this is not straightforward to demonstrate using a conventional ITO-coated glass cell since an in-plane electric field is required. For this to be realised, interdigitated electrodes are needed and, while it allows for an analogue control of the emission wavelength, due to the inhomogeneous electric field profile it can cause a degradation of the band gap, resulting in multiple modes in the emission spectrum. Ultimately, this can lead to the cessation of laser emission at large electric field amplitudes [15].

On the other hand, an electric field applied along the transverse direction of the cell (i.e. parallel to the helix axis) can lead to the CLC collapsing into a focal conic texture, this removes the PBG and so lasing is curtailed [16]. To overcome the reorientation of the CLC into focal conic domains, a number of studies have considered using reactive mesogens [18–20] to form a polymer network that 'locks-in' the uniform standing helix alignment to enhance the stability when high electric field amplitudes are applied. For example, Mohammadimasoudi, et al have shown broad tuning of a CLC PBG when very high fields (E >100 V/μm) are applied, which is believed to be due to a change in the effective refractive index of the LC in nano-sized domains [18]. Alternatively, Inoue, et al [19] have demonstrated a small degree of wavelength tuning (~ 6 nm) of a band-edge laser at similarly high electric fields (E~100s V/μm) by incorporating a dye into a polymer-stabilized network, and using the local reorientation of the LC molecules in the polymer network's nanopores to alter the refractive index.

A different approach to wavelength-tuning of the PBG has been to combine templated polymer structures with an achiral nematic LC [20]. In this case, the non-reactive chiral nematic LC molecules are washed out from the polymer scaffold and replaced with an achiral nematic LC. Using different materials filled into these scaffolds, as well as altering the refilling conditions have been shown to tune the PBG spectral position [21], however, as yet, electric-field-induced tuneable laser emission using templates has not been demonstrated. Therefore, in this work, we compare the electric field-induced spectral shift of the laser emission wavelength for a 'templated' sample with that of a conventional polymerized dye-doped chiral nematic LC. It is shown that the tuning range is more than a factor of two greater for the templated sample at the same electric field amplitudes, which is attributed to a softening of the network during the removal and subsequent refilling of the polymer scaffold with a dye-doped nematic LC. Furthermore, since the dye is added after the photo-curing process in the 'templated' system, the technique avoids problems caused by unwanted absorption and free-radical interactions with the fluorescent dye.

Experimental section

Sample preparation. In this work, two samples were used – a conventional polymerized dye-doped chiral nematic LC and a templated sample created by filling an achiral dye-doped LC

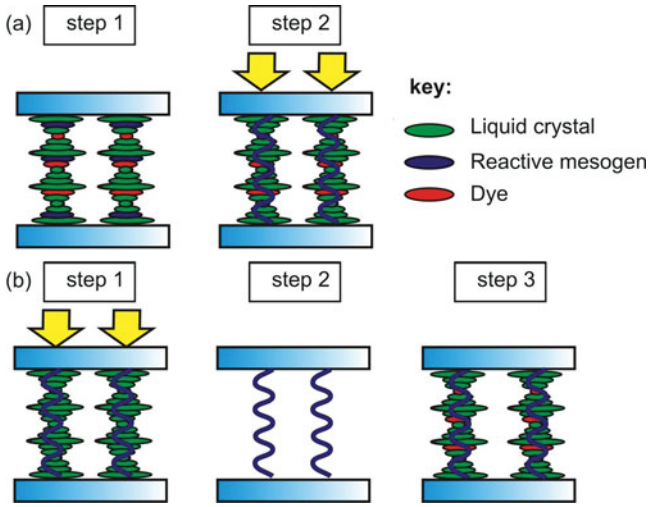

Figure 1. An illustration of the two different sample preparation techniques used in this study: a) dye-doped polymer-stabilized LC laser is created by filling a dye-doped chiral nematic LC-reactive mesogen mixture into a glass cell (step 1) and then exposed to UV light to form the polymer network (step 2); b) a templated laser is formed by photo-curing a chiral nematic LC-reactive mesogen mix using UV light (step 1), the LCand unreacted reactive mesogens are removed to leave a chiral polymer scaffold (step 2), which is then refilled with a dye-doped nematic LC (step 3).

into a scaffold created using a chiral nematic host. The achiral nematic LC used in this study was the nematogenic mixture **MDA-02-2149** (Merck), which exists in the nematic phase up to 97°C on heating, has a dielectric anisotropy of $\Delta\varepsilon = 38.5$ and a birefringence of $\Delta n = 0.18$ at T = 25 °C. This nematic mixture was chosen as it is liquid crystalline at room temperature and has a large high dielectric anisotropy. The high twisting power chiral dopant **R5011** (Merck) was dispersed into the nematic LC to form a CLC phase with a right-handed helical structure. To create a polymer network, a mixture of reactive mesogens, photoinitiator and thermal inhibiter (**UCL-011-K1**, DIC) was added to the LC host. For the results shown in this study, the fluorescent dye Pyrromethene 597 (**PM597**, Exciton) was used as a gain material as it has been shown to possess a high quantum efficiency, and therefore, low excitation energy threshold in chiral nematic LCs and, moreover, the absorption band of the dye is at longer wavelengths than the UV wavelengths used to create the polymer network [22].

Polymer-stabilized CLC laser preparation

The polymerizable CLC mixtures were made as shown in Figure 1a. Initially, the nematic LC, the chiral dopant and the UCL-011-K1 mixture were thermally mixed by heating them to above the isotropic temperature (97°C) for a period of 14 hours. PM597 was then added and the mixture was heated to the same temperature for a further 14 hours. The composition of the mixture was 67.9 wt/% MDA-02-2149, 29.1 wt/% UCL-011-K1, 2.4 wt/% R5011 and 0.6 wt/% PM597.

This was then capillary filled into 9 µm planar-aligned cells made of indium tin oxide (ITO)-coated glass consisting of anti-parallel rubbed planar alignment layers (Instec). Once a uniform standing helix texture had been achieved (as determined from optical polarizing microscope (optical polarizing microscope) images), the mixture was then photo-cured with

a UV light source ($\lambda = 365$ nm) at a temperature of 25°C as shown in Figure 1a. The samples were illuminated for 120 s from each side of the glass cell at a distance of 10 cm from a 185 mW/cm^2 high-powered LED UV-curing system (Thorlabs CS2010).

Templated laser preparation

The templated laser was made as illustrated in Figure 1b, starting from a mixture of 69.7 wt/% MDA-02-2149, 27.5 wt/% UCL-011-K1 and 2.8 wt/% R5011. The reactive mesogen concentration (≈28 wt/%) was chosen as a compromise between two competing factors. Firstly, the polymer scaffold should be robust enough to survive the washing out procedure. Secondly, the concentration should not be so high that the helix was completely locked-in, otherwise high electric fields would be required to observe tuning through the reorientation of the alignment of the LC within nanopores, as already shown in [18].

The mixture was then capillary filled into the same 9 µm planar-aligned cells that have been described previously. Once a uniform standing helix texture had been achieved (as determined from optical polarizing microscope images), the samples were then illuminated for 12 s from each side of the glass cell at a distance of 10 cm from the185 mW/cm^2 high-powered LED UV-curing system.

To remove the unreacted reactive mesogens and the CLC, the cells were placed in a beaker of acetone for 48 hours and then left to dry at room temperature for 8 hours. Optical polarizing microscope images and spectral analysis were used to confirm that the LC had been fully washed out. Following this, a dye-doped achiral mixture (99.1 wt/% MDA-02-2149 and 0.9 wt/% PM597) was then capillary-filled into the cells at 105°C, a process that took around 24 hours (i.e. much slower than capillary filling into empty cells). This is the same weight of dye as a percentage of the LC material as used in the polymerized laser samples.

Optical analysis. The transmission spectra were recorded by illuminating each sample with a broadband halogen white light source perpendicular to the substrates of the glass cell (Ocean Optics HL-2000-FHSA) and recording the transmission spectrum on a fiber-coupled universal serial bus spectrometer (Ocean Optics USB2000+ UV-VIS) with a 600 μm-diameter fiber and a resolution of 1.7 nm. An Olympus BX51 optical polarizing microscope with a camera (QICam Fast1394) attached to the photo-tube was used to check the alignment of the LC samples and to record images of the optical textures.

Optical pumping. The devices were optically pumped with a frequency-doubled Nd:YAG laser (CryLas 6FTSS355-Q4-S) emitting 1 ns-pulses at 532 nm with a repetition rate of 10 Hz. The pump laser was focused onto the devices using a focusing lens to a spot size with a diameter of approximately 200 μm and then the output was collected perpendicular to the device using a series of collection optics. A 550 nm long pass filter was inserted after the sample and before the spectrometer to block the pump beam from being detected. Emission from the LC sample was collected using an objective (N.A. = 0.25) and coupled into the 600 µm-diameter fiber attached to the spectrometer.

Electric field analysis. A voltage was applied across the glass cells using two out-of-phase 1 kHz square wave signal generators (Tektronix AFG-3022). To obtain voltages up to 400 $V_{p\text{-}p}$ (22.2 V/µm for 9 µm cells) a voltage amplifier (FCC electronics F10AP) was required. The output from the amplifier was monitored using a digitizing oscilloscope (Tektronix TDS224).

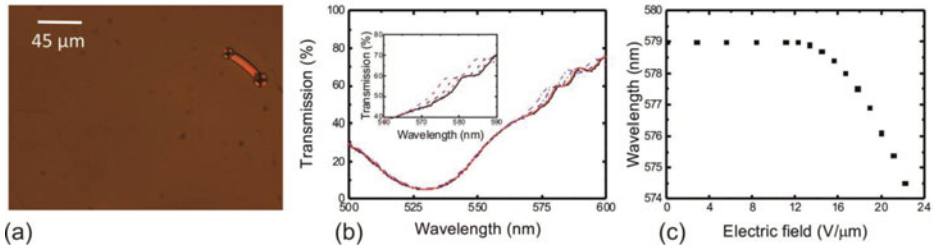

Figure 2. Wavelength tuning of a dye-doped polymer-stabilized chiral nematic LC: a) an optical polarizing microscope image of the Grandjean alignment after photo-curing. Two spacer beads (9 µm diameter) and an oily streak can be seen in the top right; b) The change in the transmission spectrum as an electric field is applied (0, 15.6, 20, 22.2 V/μm from right to left) and c) The wavelength of the center of the LBE as a function of the applied electric field amplitude.

Results and discussion

Polymer stabilized samples

Figure 2a shows an optical polarizing microscope image of the polymer-stabilized dye-doped CLC mixture after photo-curing. Subsequent electro-optic studies revealed that when an electric field was applied to the cell parallel to the axis of the helix, the PBG was retained even at the highest electric field strength achievable with our experimental setup (22.2 V/µm). Figure 2b presents results of the transmission spectra of the device when illuminated by a white light source for several different electric field amplitudes up to the maximum of E = 22.2 V/µm, where it can be seen that there is a slight blue-shift of the long-wavelength band-edge on increasing the electric field amplitude. In this case the short-wavelength band-edge is masked by the absorption of the laser dye (the peak absorption occurs at 530 nm).

The long-wavelength band-edge (LBE) on increasing the electric field amplitude is plotted in Figure 2c. Here, the results show that there is almost no movement of the band-edge up until an electric-field of E = 12 V/µm before a blue shift in the wavelength is observed. Above that field amplitude, the wavelength of the LBE appears to shift continuously with a further increase in the electric field resulting in a total blue-shift of ≈ 4.5 nm. These results are in contrast to that observed for the case of a dye-doped chiral nematic LC sample that was not polymer-stabilized whereby the standing helix alignment would collapse before any tuning was seen and the PBG observed along the normal of the cell substrates appeared to vanish at E ≈1 V/µm.

The sample was then optically pumped with the second harmonic of a Nd:YAG laser and laser emission was observed along the normal of the cell substrates at a wavelength corresponding to the LBE. The emission spectrum was found to be slightly broader than the resolution limit of the spectrometer (1.7 nm). This is likely due to inhomogeneities in the polymeric structure caused by the presence of the dye during curing, resulting in a multimode laser output. Figure 3a shows examples of the emission spectrum for different electric field amplitudes indicating that the peak laser wavelength is blue-shifted as the magnitude of the electric field increases. This is in accordance with the blue-shift of the band-gap observed in the transmission spectrum (c.f. Figure 2b). Thus, the wavelength tuning-range of the peak laser wavelength was ≈4.5 nm, as shown clearly in Figure 3b and is commensurate with the data presented in Figure 2c. A plot of the input-output characteristics of the laser sample showing the peak output intensity as a function of the excitation energy per pulse is presented in

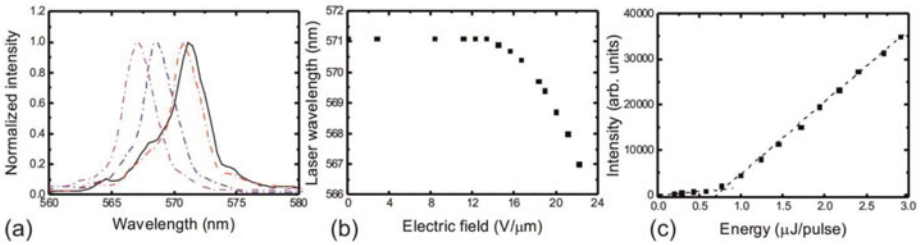

Figure 3. Wavelength tuning of the emission from a dye-doped polymer-stabilized chiral nematic LC: a) emission spectra for four different electric field amplitudes (0, 15.6, 20, 22.2 V/μm from right to left); b) Peak wavelength as a function of the applied electric field amplitude and c) laser peak intensity as a function of the excitation energy per pulse.

Figure 3c, from the discontinuity in the differential we estimate the threshold of the laser to be $E_{th} \approx 0.75$ μJ/cm^2.

Polymer templated LC lasers

The same experiments were then performed using the polymer template that had been refilled with a dye-doped nematic LC. Figure 4a shows an optical polarizing microscope image of the alignment of the CLC. Although slightly more domains are apparent, which are separated by oily streaks, the domains are of the same color, indicating that the pitch is the same. The texture does not change upon rotating the sample between crossed-polarizers indicating a Grandjean alignment. Therefore, even though there are more defects present than before the removal of the unreacted chiral nematic LC, it still exhibits good alignment after being refilled and the PBG is found to reappear. Again, when an electric field was applied, the PBG was retained even up to a field of E = 22.2 V/μm – shown in Figure 4b. However, for this sample, the LBE was found to shift by 11 nm (Figure 4c) for the same electric field amplitude, which is more than a factor of two greater than that observed for the polymer-stabilized sample.

Similarly, the wavelength shift was mirrored in the laser emission spectra: Figure 5a shows the laser emission spectrum for four different electric field strengths. The laser spectra have a narrower linewidth in this case indicating a more uniform periodic structure. This is believed to be a result of the dye not being present during the photo-curing process, which may adversely interfere with the morphology and formation of the polymer network. Figure 5b

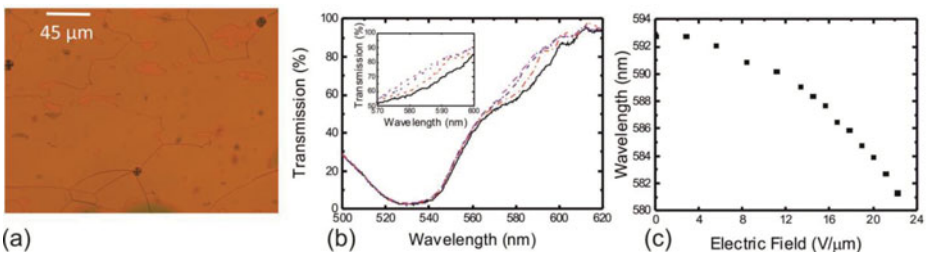

Figure 4. Wavelength tuning of the LBE for a dye-doped nematic LC in a chiral polymer scaffold: a) an optical polarizing microscope image of the optical texture after refilling the polymer template with a dye-doped nematic LC showing the reappearance of the Grandjean texture. The black dots are spacer beads (9 μm diameter); b) The change in LBE of the band-gap on increasing the applied electric field amplitude (0, 15.6, 20, 22.2 V/μm from right to left) and c) The wavelength of the LBE as a function of the applied electric field amplitude.

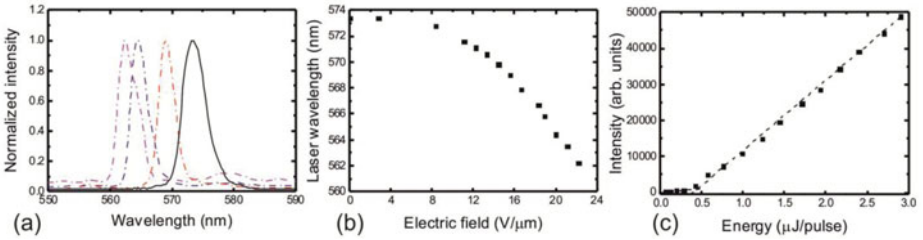

Figure 5. Laser emission from a dye-doped nematic LC in a chiral polymer scaffold: a) the laser emission spectrum for four different applied electric field amplitudes (0, 15.6, 20, 22.2 V/μm from right to left); b) Peak laser wavelength as a function of the applied electric field; c) laser peak intensity as a function of the excitation energy per pulse.

shows the change in peak laser wavelength as the amplitude of the electric field increases. Again, a blue-shift of $\Delta\lambda_{LBE} \approx 11$ nm is observed. The excitation threshold, extracted from the input-output plot shown in Figure 5c, is found to be somewhat lower than for the polymer-stabilized laser sample presented in Figure 3 ($E_{th} \approx 0.5$ μJ/cm^2). This could be due to either a reduction of the quantum efficiency of the dye in the presence of the unreacted free-radicals or due to increased losses as a result of the inhomogeneous polymer morphology in the polymer-stabilized sample where the dye is present during the photo-curing procedure.

Collectively, these results show that the templating and refilling process appears to enhance the wavelength tuning range of a CLC laser. We believe that the blue-shift observed in Figures 2 and 3 is due to tilting of the molecules within the helix so as to align with the direction of the applied field. Furthermore, we assume that the pitch is fixed by the polymer network and that the electric field induces a change in the effective value of n_e, which in turn results in a decrease in λ_L. According to Eq. 1, we estimate that the change in the refractive index is very small, of the order of 0.01, for a 4 nm blue shift. Much larger tuning ranges are likely to be achieved if higher electric field amplitudes can be accessed. For example, using our setup but with thinner cells, the tuning-range of the LBE was much enhanced. However, to provide sufficient feedback to support laser emission, the device thickness must be above a minimum value [23]. For the template sample, we believe that another mechanism is acting to allow the greater wavelength shift on refilling and that the additional tuning may be the result of a softening of the network. Further studies are currently underway to gain a deeper understanding of the mechanisms that underpin wavelength-tuning in these devices.

In conclusion, by refilling a polymer template of a CLC with a fluorescent dye-doped, achiral nematic LC, we have shown that the laser wavelength can be tuned using external electric fields over a greater range than that observed for a conventional polymer-stabilized CLC. Moreover, the refilling technique also circumvents problems associated with photo-polymerization in the presence of a fluorescent dye, which can interfere with the formation of the polymer network and lead to free-radical-dye interactions that lead to non-radiative pathways.

Acknowledgments

SMM gratefully acknowledges the financial support of The Royal Society and SMW acknowledges the EPSRC for a Studentship.

References

[1] Kim, K.-H., & Song, J.-K. (2009). *NPG Asia Mater.*, *1*, 1.
[2] Woltman, S. J., Jay, G. D., & Kasano, M. (2007). *Nat. Mater.*, *6*, 929.
[3] Coles, H., & Morris, S. (2010). *Nat. Photonics*, *4*, 10.
[4] Kasano, M., Ozaki, M., Yoshino, K., Ganzke, D., & Haase, W. (2003). *Appl. Phys. Lett.*, *82*, 4026.
[5] Cao, W., Muñoz, A., Palffy-Muhoray, P., & Taheri, B. (2002). *Nat. Mater.*, *1*, 111.
[6] Yokoyama, S., Mashiko, S., Kikuchi, H., Uchida, K., & Nagamura, T. (2006). *Adv. Mater.*, *18*, 48.
[7] Dowling, J. P., Scalora, M., Bloemer, M. J., & Bowden, C. M. (1994). *J. Appl. Phys.*, *75*, 1896.
[8] de Vries, H. (1951). *Acta Crystallogr.*, *4*, 3.
[9] Schmidtke, J., & Stille, W. (2003). *Eur. Phys. J. B - Condens. Matter*, *31*, 2.
[10] John, S. (1987). *Phys. Rev. Lett.*, *58*, 2486.
[11] Funamoto, K., Ozaki, M., & Yoshino, K. (2003). *Jpn. J. Appl. Phys.*, *42*, 12B.
[12] Lelidis, I., Barbero, G., & Scarfone, A. M. (2012). *Cent. Eur. J. Phys.*, *10*, 3.
[13] Finkelmann, H., Kim, S. T., Muñoz, A., Palffy-Muhoray, P., & Taheri, B. (2001). *Adv. Mater.*, *13*, 14.
[14] Furumi, S., Yokoyama, S., Otomo, A., & Mashiko, S. (2003). *Appl. Phys. Lett.*, *82*, 1.
[15] Schmidtke, J., Juünnemann, G., Keuker-Baumann, S., & Kitzerow, H.-S. (2012). *Appl. Phys. Lett.*, *101*, 5.
[16] Choi, S., Morris, S. M., Huck, W. T. S., & Coles, H. J. (2009). *Adv. Mater.*, *21*, 3915.
[17] Yang, D.-K., West, J. L., Chen, L. C., Doane, J. W. (1994). *J. Appl. Phys.*, *76*, 1331.
[18] Mohammadimasoudi, M., Beeckman, J., Shin, J., Lee, K., & Neyts, K. (2014). *Opt. Express*, *22*, 19098.
[19] Inoue, Y., Yoshida, H., Inoue, K., Shiozaki, Y., Kubo, H., Fujii, A., & Ozaki, M. (2011). *Adv. Mater.*, *23*, 46.
[20] Choi, S. S., Morris, S. M., Huck, W. T. S., & Coles, H. J. (2010). *Adv. Mater.*, *22*, 1.
[21] Lin, J.-D., Chu, C.-L., Lin, H.-Y., You, B., Horng, C.-T., Huang, S.-Y., Mo, T.-S., Huang, C.-Y., & Lee, C.-R. (2015). *Opt. Mater. Express*, *5*, 1419.
[22] Mowatt, C., Morris, S. M., Song, M. H., Wilkinson, T. D., Friend, R. H., & Coles, H. J. (2010). *J. Appl. Phys.*, *107*, 043101.
[23] Mavrogordatos, T. K., Morris, S. M., Castles, F., Hands, P. J. W., Ford, A. D., Coles, H. J., & Wilkinson, T. D. (2012). *Phys. Rev. E*, *86*, 11705.